AGU PUBLICATIONS

JGR

Journal of Geophysical Research: Solid Earth

RESEARCH ARTICLE
10.1002/2014JB011118

Key Points:
- Daily and seasonal cycles are identified in CO_2 efflux in volcanic areas
- Water table and thermal amplitudes are explicative factors of diurnal cycles

Supporting Information:
- Readme
- Table S1
- Table S2
- Table S3
- Table S4
- Table S5
- Figure S1
- Figure S2
- Figure S3

Correspondence to:
F. Viveiros,
Maria.FB.Viveiros@azores.gov.pt

Citation:
Viveiros, F., J. Vandemeulebrouck, A. P. Rinaldi, T. Ferreira, C. Silva, and J. V. Cruz (2014), Periodic behavior of soil CO_2 emissions in diffuse degassing areas of the Azores archipelago: Application to seismovolcanic monitoring, *J. Geophys. Res. Solid Earth*, *119*, doi:10.1002/2014JB011118.

Received 13 MAR 2014
Accepted 26 SEP 2014
Accepted article online 1 OCT 2014

Periodic behavior of soil CO_2 emissions in diffuse degassing areas of the Azores archipelago: Application to seismovolcanic monitoring

Fátima Viveiros[1], Jean Vandemeulebrouck[2], Antonio P. Rinaldi[3], Teresa Ferreira[1], Catarina Silva[1], and José V. Cruz[1]

[1]Centro de Vulcanologia e Avaliação de Riscos Geológicos, Universidade dos Açores, Ponta Delgada, Portugal, [2]ISTerre, Université de Savoie, CNRS, Chambery, France, [3]Earth Sciences Division, Lawrence Berkeley National Laboratory, Berkeley, California, USA

Abstract Time series of soil CO_2 efflux recorded in the Azores archipelago volcanic-hydrothermal areas feature daily and seasonal variations. The recorded CO_2 efflux values were lower during summer than in the winter season. The diurnal CO_2 efflux values were higher at dawn and lower in the early afternoon, contrary to that observed in biogenic environments. CO_2 efflux cycles correlated well with the environmental variables, such as air temperature, wind speed, and barometric pressure, which also showed low- and high-frequency periodicities. Several simulations were performed here using the Transport of Unsaturated Groundwater and Heat 2 (TOUGH2) geothermal simulator to complement the study of Rinaldi et al. (2012). The effects of the water table depth, air temperature perturbation amplitude, and soil thermal gradient contributed to an explanation of the contrasts observed in the diurnal (S_1) and semidiurnal (S_2) soil CO_2 efflux peaks for the different monitoring sites and seasons. Filtering techniques (multivariate regression analysis and fast Fourier transform filters) were also applied to the recorded time series to remove effects of external variables on the soil CO_2 efflux. The resulting time series (the residuals) correspond to the best approach to the deep-seated (volcanic/hydrothermal) CO_2 emissions and thus should be used in seismovolcanic monitoring programs. Even if no evident correlation can be established yet between the soil CO_2 residuals and seismicity over the monitored time, a seismic swarm that occurred around the end of 2008 might have triggered some deviations from the observed daily cycles.

1. Introduction

Environmental variables have been shown to greatly influence soil gas emissions in several areas [e.g., *Cigolini et al.*, 2009; *Chiodini et al.*, 1998; *Clements and Wilkening*, 1974; *Granieri et al.*, 2003, 2010; *Hinkle*, 1990, 1994; *Klusman and Webster*, 1981; *Lewicki et al.*, 2007; *Perrier and Girault*, 2013; *Rinaldi et al.*, 2012; *Viveiros et al.*, 2008, 2009]. Notwithstanding the influence of the physical properties of the soil on the gas efflux, and in addition to barometric pressure and wind, the most important environmental variables that influence soil degassing are rainfall, snowfall, soil moisture, soil temperature, and air temperature [e.g., *Carapezza et al.*, 2009; *Chiodini et al.*, 1998; *Granieri et al.*, 2003, 2010; *Hinkle*, 1991, 1994; *Klusman et al.*, 2000; *Lewicki et al.*, 2007; *Pinault and Baubron*, 1996; *Viveiros et al.*, 2008]. Several studies performed in different degassing areas have shown that environmental variables can have great influence on the rate of gas released from the soil. Some studies have estimated that variations in diffuse emissions of up to ±50% of the average CO_2 efflux are due to environmental changes only (e.g., barometric pressure, wind speed, and rainfall) [*Rogie et al.*, 2001; *Viveiros et al.*, 2008]. The impact of environmental variables on gas efflux clearly depends on the monitored site [e.g., *Viveiros et al.*, 2008], even though the interference of external variables with degassing can also vary at the same site over long time series, as has been observed at a permanent CO_2 efflux station at Solfatara volcano (Campi Flegrei, Italy) [*Granieri et al.*, 2003, 2010]. The correlations between environmental parameters and soil gas variations thus need to be understood and quantified, to be able to discriminate between meteorological effects and changes in deep-seated volcanic/hydrothermal sources.

The first relationships established between soil CO_2 and environmental conditions were obtained for biogenic CO_2 [e.g., *Witkamp*, 1969], and it was only in the early 1990s that CO_2 degassing from deep origins was studied in detail and correlated with external factors [e.g., *Chiodini et al.*, 1998; *Hinkle*, 1990, 1994]. Diurnal and seasonal variations of biogenic soil CO_2 efflux derived from soil respiration mainly correlate with atmospheric cycles [e.g., *Bajracharya et al.*, 2000; *Maier et al.*, 2010; *Nakadai et al.*, 2002; *Witkamp*, 1969]. In some studies

©2014. American Geophysical Union. All Rights Reserved.

cyclic variations in ^{222}Rn time series have also been identified, both in the air [e.g., *Groves-Kirkby et al*., 2006; *Pinault and Baubron*, 1997; *Richon et al*., 2009; *Rigby and La Pointe*, 1993; *Robinson et al*., 1997; *Steinitz et al*., 2007] and in the soil [*Aumento*, 2002; *Cigolini et al*., 2009; *Perrier and Girault*, 2013; *Richon et al*., 2003, 2011]. However, despite the recognized influence of environmental conditions on the CO_2 efflux behavior, there are only a few studies in the literature that have reported daily variations in soil CO_2 emitted from volcanic/hydrothermal areas [*Granieri et al*., 2003; *Padrón et al*., 2008; *Hernández et al*., 2012]. Recently, *Rinaldi et al*. [2012] simulated the influence of air temperature and barometric pressure on the gas flux through the dry season, and they showed a significant correlation between these two factors and the semidiurnal and diurnal cycles (12 h and 24 h, respectively). In addition, this influence was studied for varying soil permeability and gas reservoir overpressure. Results indicated that permeability enhancement causes similar changes in the 12 h and 24 h components, while increases in the gas reservoir overpressure produce different behaviors of these two components.

In addition to diurnal periodicities, annual cycles have also been recognized in CO_2 emissions at the Furnas and Fogo volcanoes (Azores) and at Solfatara, where higher CO_2 effluxes were recorded during the rainy seasons [*Granieri et al*., 2010; *Viveiros*, 2010; *Viveiros et al*., 2008]. Recently, spectral analysis was also applied to a SO_2 flux time series recorded at Soufrière Hills Volcano (Montserrat, United Kingdom) [*Nicholson et al*., 2013], which showed cycles on multiyear and multiweek timescales.

Environmental factors have been shown to control not only near-surface processes but also deeper phenomena, even if the source mechanisms are not well understood yet. *Marzocchi et al*. [2001] detected 24 h periodicities in earthquake sequences at Campi Flegrei and Vesuvius volcanoes (Italy) that were tentatively correlated with thermal diurnal processes. *López et al*. [2006] showed the influence of the Earth tides in degassing and volcanic tremor in the Arenal Volcano (Costa Rica). *Patanè et al*. [2007] noted possible meteorological influences on the Stromboli magmatic system (Italy) during the 2007 eruption. Some seasonal effects in the velocity patterns of seismic waves were also detected for Fogo Volcano (Azores) and were correlated with episodes of abundant rainfall [*Martini et al*., 2009]. These correlations established between deep-sourced phenomena (e.g., earthquakes and magmatic activity) and external variations confirm the importance of the inclusion of environmental conditions in any seismovolcanic monitoring program.

In the present study, spectral analysis was applied to long CO_2 efflux time series recorded at three permanent gas stations installed at Furnas Volcano (between 2002 and 2009) to identify and characterize the daily and seasonal periodic patterns. In addition, and for monitoring purposes, statistical filters were applied to the CO_2 efflux time series, to remove the environmental effects and to compute the residuals, which likely originate from deeper volcanic/hydrothermal sources. Compared to the *Rinaldi et al*. [2012] study, the present study highlights the differences observed in the periodic components when considering the effects of different seasons and different monitoring sites. Simulations were performed to account for parameters such as water saturation (which is related to the water table depth) and air temperature amplitudes to infer seasonal effects on degassing. The soil temperature gradient and temperature of the reservoir, as well as the gas overpressure, were varied, to account for the existing conditions at different monitoring sites.

2. Characterization of the Study Area

The Azores archipelago is composed of nine volcanic islands that are located in the North Atlantic Ocean in the triple junction domain of the American, Eurasian, and Nubian plates [e.g., *Searle*, 1980]. These islands are the emerged heights of various volcanic ridges that overlap in the Azores Plateau, which is an area of anomalous oceanic crust thickening. Present-day volcanic activity in the Azores archipelago features boiling temperature fumaroles, steaming ground, thermal springs, cold CO_2-rich springs, and diffuse degassing areas [*Cruz et al*., 2010; *Ferreira et al*., 2005]. Furnas Volcano is a quiescent polygenetic volcano that is located on the eastern part of São Miguel Island, and it comprises all of these surface hydrothermal manifestations. The volcanic activity of Furnas Volcano has been characterized by several eruptive styles, which have ranged from mideffusive activity to caldera-forming explosive events [*Guest et al*., 1999], and the last two subplinian phreatomagmatic eruptions occurred after settlement in the fifteenth century (1439–1443; 1630) [*Cole et al*., 1995]. Most of the secondary manifestations of volcanism are located inside the caldera, and the main diffuse degassing areas are mostly associated with visible hydrothermal manifestations showing that in these areas CO_2 is carried by the steam upflow (Figure 1). Important diffuse degassing structures (DDSs) [*Chiodini et al*., 2001] have also been found in depressed areas on the slopes of some crater/caldera rims, due to strong morphostructural control on the gas release [*Viveiros et al*., 2010].

©2014. American Geophysical Union. All Rights Reserved.

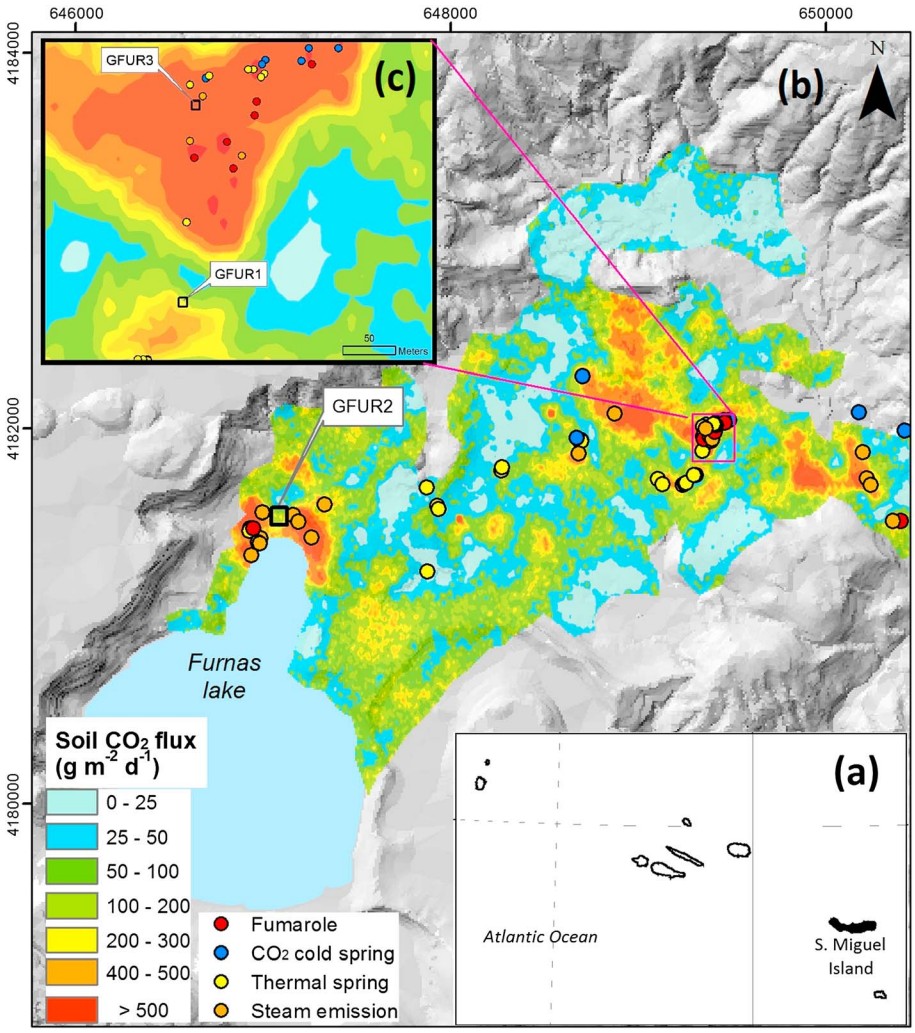

Figure 1. Location of the permanent gas flux stations. (a) Azores archipelago with São Miguel Island (black). (b) Soil CO_2 degassing map for the Furnas caldera with the main hydrothermal manifestations according to the study of *Viveiros et al.* [2010]. (c) Detailed CO_2 degassing map for the Furnas village fumarolic field. Black squares, the permanent CO_2 efflux stations.

Since 2002, the central region of São Miguel Island, which mainly comprises Fogo Volcano and Achada das Furnas Plateau (west of Furnas Volcano), has experienced higher seismic activity than in previous decades [*Silva et al.*, 2012]. In the case of the Furnas Volcano seismogenic area, the activity has been characterized by low-level seismicity with some sporadic low-magnitude seismic swarms [*Silva et al.*, 2004]. Between 2002 and 2006, less than 100 seismic events per year occurred in this seismogenic area; however, more recently, the number of events has increased slightly because of two seismic swarms that occurred in May 2007 and November 2008. Between 2002 and 2009, the maximum calculated duration magnitudes (M_D) for events located within the Furnas caldera were 2.7 and 2.6 on 2 February 2005 and on 4 November 2006, respectively (data collected by CIVISA/CVARG, http://www.cvarg.azores.gov.pt/paginas/sismicidade.aspx).

From a meteorological point of view, the Azores climate is oceanic temperate, because of the interaction between the Atlantic Ocean and a branch of the Gulf Stream that crosses the archipelago. The mean annual precipitation is 1930 mm/yr, which exceeds by far the mean annual actual evapotranspiration (581 mm/yr) [*DROTRH/INAG*, 2001]. Moreover, the Azores islands are marked by several local microclimates, which depend on factors such as altitude, distance from the sea, shape of the islands, and soil occupation [*Bettencourt*, 1979]. Several studies have highlighted the interannual and interseasonal high variability of the rainfall patterns [*Bettencourt*, 1979; *Marques et al.*, 2007]. These have shown significant differences between the "rainy season" that extends from October to March (with about 70% of the annual precipitation) and the "dry season," with the

©2014. American Geophysical Union. All Rights Reserved.

Table 1. Characterization of the Permanent CO_2 Efflux Station Sites[a]

Parameters		Station Reference GFUR1	GFUR2	GFUR3
Porosity (*n*) %		n.m.	64	61
Specific gravity (G_s)		n.m.	2.34	2.44
Hydraulic conductivity (K_{sat}) m s^{-1}		n.m.	3.72×10^{-5}	6.18×10^{-5}
Soil temperature °C	Winter	15.4	19.7	28.2
	Summer	19.8	22.5	45.8
Soil water content %	Winter	24.9	22.2	15.3
	Summer	19.3	16.9	10.7

[a]The soil temperature and soil water content (30 cm depth) correspond to the means recorded in the stations since their installation. The hydraulic conductivity was obtained by the constant head soil permeameter [*Stolte*, 1997], the specific gravity of the soil was evaluated using the pycnometer method (LNEC, NP-83, 1988), and the soil porosity (*n*) was determined by the mathematical relationships between the mass and the soil volume. Not measured: n.m.

minimum rainfall in July. The mean annual temperature of the study area varies from 14°C inside the caldera to 18°C on the southern flank. The mean annual relative air humidity exceeds 80% for the whole Furnas geographical area (Climate and Meteorology of the Atlantic Archipelagos (CLIMAAT), University of the Azores, http://www.climaat.angra.uac.pt/).

3. The Permanent CO_2 Efflux Network

The permanent soil CO_2 diffuse degassing monitoring program started in the archipelago in October 2001 with the installation of the first permanent soil CO_2 efflux station within the Furnas caldera (named GFUR1). Currently, there are two such stations installed in the Furnas caldera (São Miguel Island), which record hourly data (Figure 1).

The permanent soil gas flux stations installed in the Azores archipelago perform measurements based on the "time 0, depth 0" accumulation chamber method [*Chiodini et al.*, 1998]. Every hour, a chamber is lowered to the ground and the gas is pumped into an infrared gas analyzer. The soil CO_2 efflux is computed as the linear best fit of the flux curve over a predefined period of time. The automatic stations also have coupled meteorological and soil sensors, which simultaneously acquire data related to barometric pressure, air and soil temperatures, relative air humidity, wind speed and direction, rainfall, and soil water content.

3.1. Characterization of the Monitoring Sites

Station GFUR1 was running between October 2001 and July 2006 in a garden adjacent to the Furnas Village fumarolic field where no thermal anomaly was recorded (mean temperature at about 30 cm depth was 17.5°C). The soil CO_2 efflux values during this period oscillated around a mean of 267 g m^{-2} d^{-1}. This station was then installed in a new site within the Furnas Village fumarolic field area in January 2008 (when it was renamed as GFUR3), where CO_2 efflux values of approximately 650 g m^{-2} d^{-1} were measured. This new monitoring site also showed a thermal anomaly, with a mean soil temperature of 37°C at 30 cm depth (Table 1). A second soil CO_2 efflux station, named GFUR2, was also installed inside the Furnas caldera in October 2004, in the surroundings of Furnas Lake fumarolic area, where soil CO_2 efflux and temperatures around 350 g m^{-2} d^{-1} and 22°C, respectively, were measured. These stations were installed over identified DDS, which confirms that the CO_2 efflux is mainly fed by the hydrothermal source [*Viveiros et al.*, 2010]. The deep origin of the CO_2 for these monitoring sites is also confirmed by the isotopic compositions of the CO_2 efflux ($\delta^{13}C_{CO2}$), which are −6.16‰ and −4.39‰ for sites GFUR2 and GFUR3, respectively [*Viveiros et al.*, 2010]. The mean soil temperature at about 30 cm depth was significantly higher during the summer months, essentially in the thermally anomalous zones (site GFUR3), contrary to the soil water content, which was higher in winter periods (Table 1). The water table depth at site GFUR2 was about 1 m, due to the proximity of the lake and its level close to the ground surface. Even if no detailed information is available for the water table depth at sites GFUR1 and GFUR3, it should be deeper than at GFUR2 considering the topographic position of these two stations in a slightly elevated area.

A general characterization of the topsoils of the GFUR2 and GFUR3 monitoring sites was performed by *Viveiros* [2010], to address differences in the physical properties of the soils (mostly porosity and hydraulic conductivity, Table 1) that might explain the different influences of the environmental variables on the CO_2

©2014. American Geophysical Union. All Rights Reserved.

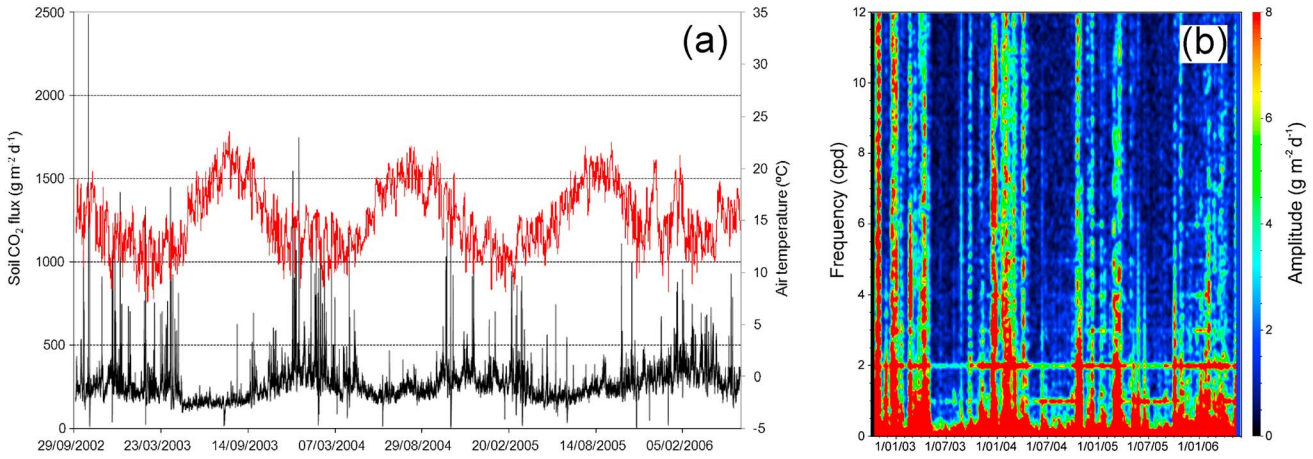

Figure 2. Time series recorded at station GFUR1 and the associated spectrogram. (a) Soil CO_2 efflux (black) and air temperature (red) recorded at GFUR1 from 2 October 2002 to 31 May 2006. (b) Spectrogram of the soil CO_2 efflux recorded at site GFUR1 for the same period.

efflux. Such data are not available for site GFUR1 as the surveys were carried out in 2008 only, and the area where GFUR1 was previously installed had been cemented over.

Analysis of the soil samples collected at the Furnas Volcano highlights the relatively similar physical properties for monitoring sites GFUR2 and GFUR3. These similarities are probably due to the pumice volcanic materials from the latest explosive eruption, which covered the caldera floor and constitute the unaltered raw material that makes up the soil. Moreover, the meteorological factors that affect the soil are similar for both of these stations, because of their geographic proximity. The above mentioned physical properties of the soils are similar to those measured for other pumice soils, as is the case for the deposits associated with the explosive activity of the Somma-Vesuvius volcanic system (Italy) [*Crosta and Dal Negro*, 2003; *Esposito and Guadagno*, 1998]. The soil surface is covered with grass at GFUR2 (as it was for GFUR1). For GFUR3, which is located in a thermally anomalous zone, the soil is poorly vegetated.

4. Data Analysis and Results

The data analyzed in this study were collected from March 2002 to May 2006 at station GFUR1 and from January 2005 to June 2009 at the monitoring site GFUR2. For GFUR3, the period under study was shorter, as from August 2009 to March 2010. The soil CO_2 efflux recorded at station GFUR1 ranged between 2 and 2486 g m^{-2} d^{-1}, with a mean value of 267 g m^{-2} d^{-1}. At station GFUR2, the CO_2 efflux varied between 7 and 907 g m^{-2} d^{-1}, with a mean of 398 g m^{-2} d^{-1} (Figures 2a and 3a). For GFUR3, the soil CO_2 efflux varied between 119 and 722 g m^{-2} d^{-1} with a mean of 363 g m^{-2} d^{-1}.

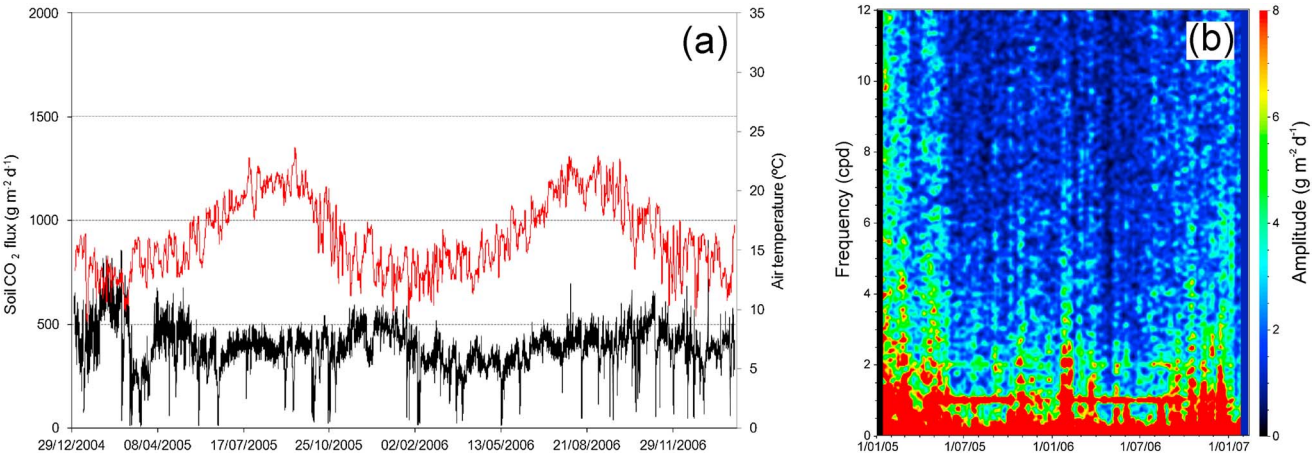

Figure 3. Time series recorded at station GFUR2 and the associated spectrogram. (a) Soil CO_2 efflux (black) and air temperature (red) recorded at GFUR2 from 1 January 2005 to 9 February 2007. (b) Spectrogram of the soil CO_2 efflux values recorded at site GFUR2 for the same period.

©2014. American Geophysical Union. All Rights Reserved.

4.1. Regression Analysis Applied to the Data Acquired

Both spike-like and long-term oscillations were identified in the CO_2 efflux time series recorded at the Furnas permanent stations [*Rinaldi et al*., 2012; *Viveiros et al*., 2008; *Viveiros*, 2010]. In previous studies, multivariate regression analysis (MRA) was applied to the data. Results showed that the monitored environmental variables can explain between 39.5% and 50.5% of the soil CO_2 efflux variations at the stations installed within the Furnas caldera, causing several spiky variations. The variables that showed statistical significance in explaining the soil CO_2 efflux variations were barometric pressure, wind speed, rainfall, soil water content, soil temperature, and air temperature, as observed from regression equations (1) to (3) [*Viveiros et al*., 2008; *Viveiros*, 2010],

$$q^{CO_2}_{GFUR1} = 5509.84 + 3.65W - 5.05p_{atm} - 16.49T_{soil} + 28.5r - 0.62r^2 + R \quad (1)$$

$$q^{CO_2}_{GFUR2} = -1555.30 + 20.28T_{soil} - 8.17T_{air} + 1.41p_{atm} - 0.64W^2 - 5.76r - 10.92w + 26.9W^2 + R \quad (2)$$

$$q^{CO_2}_{GFUR1} = 2029.35 + 24.96T_{soil} - 2.11p_{atm} - 28.08w - 2.96T_{air} - 0.28T^2_{soil} + R \quad (3)$$

where q is the soil CO_2 efflux at each of the three stations, W is the soil water content, p_{atm} is the barometric pressure, T_{soil} and T_{air} are the soil and air temperatures, respectively, r is the amount of rain, w is the wind speed, and R represents the residuals.

Previous studies have also used MRA to filter out the influence of the environmental variables on the soil CO_2 efflux [*Granieri et al*., 2003, 2010; *Viveiros et al*., 2008]. Application of this statistical methodology allows computation of a new time series, the residuals, which correspond to the CO_2 variations that are not explained by the monitored variables that were introduced in the regression model. Consequently, the residuals represent variations in the deep-sourced gas flow, and the corresponding time series should be integrated into any seismovolcanic monitoring program. A previous study performed with Furnas Volcano geochemical data did not show any direct relationship between CO_2 efflux residuals and the seismic activity recorded for the Furnas seismogenic area, probably because of the low magnitude of the earthquakes recorded in the area [*Viveiros et al*., 2008].

4.2. Spectral Analysis Applied to the Recorded Time Series

To identify harmonic oscillations, the data sets recorded by the permanent soil CO_2 efflux stations were analyzed using the freely distributed *Tsoft* software, version 2.1.2 [*Van Camp and Vauterin*, 2005; *Vauterin and Van Camp*, 2008] (Tsoft manual, http://seismologie.oma.be/TSOFT/tsoft.html).

Considering that the results are influenced by the lengths of the data sets and by any gaps, the time series were reviewed, with insertion of the missing values as the means of the nearby points (when only a few values were missing in the gaps). The fast Fourier transform (FFT) spectra of the different recorded time series were calculated, as well as the moving window spectrum, to analyze spectral variations versus time. To minimize spectral leakage, a Hanning window was selected, forcing the endpoints to zero [*Harris*, 1978]. A transfer function between two selected time series was also performed by moving the FFT on two channels to allow assessment of the correlation coefficients and the time delay between the time series [*Van Camp and Vauterin*, 2005; *Vauterin and Van Camp*, 2008].

4.3. Results

4.3.1. Diurnal Variations

4.3.1.1. The GFUR1 Data

Daily cycles are observed in the soil CO_2 efflux time series recorded at GFUR1 (Figure 2b). Two dominant spectral peaks are observed at 1 cycle per day (cpd) and 2 cpd, which represent the diurnal (24 h, S_1) and semidiurnal (12 h, S_2) cyclic components, respectively. Other low-energy peaks with 3 cpd, 4 cpd, and 5 cpd also appear in the spectrogram.

The spectrogram shows some spots with prevailing cycles, which makes it possible to observe a stronger and more evident 2 cpd frequency during the winter months (November to April), compared to the summer months (May to September). Based on the seasonal variations observed at the 1 and 2 cpd frequencies, the amplitude spectra of the data acquired during the different seasons were also calculated. On the one hand, the ratios between the S_1 and S_2 peaks show that only the 12 h component is observed in the soil CO_2 efflux

©2014. American Geophysical Union. All Rights Reserved.

Table 2. S_1/S_2 Amplitudes of the Soil CO_2 Efflux and Some Environmental Data Recorded at Station GFUR1 for the Specified Periods

Variable	Period	S_1/S_2
Soil CO_2 efflux (g m^{-2} d^{-1})	2 October 2002 to 31 May 2006	0.5
Air temperature (°C)		3.1
Barometric pressure (hPa)		0.3
Soil CO_2 efflux (g m^{-2} d^{-1})	Summer months (2003–2005)	1.8
Air temperature (°C)		4.9
Barometric pressure (hPa)		0.6
Soil CO_2 efflux (g m^{-2} d^{-1})	Winter months (2002–2006)	S_2 only
Air temperature (°C)		2
Barometric pressure (hPa)		S_2 only

spectrum during the winter months (Table 2), which is in agreement with observations obtained from the spectrograms. On the other hand, during the summer months, 1 cpd and 2 cpd frequencies are detected, with the amplitude of the S_1 peak slightly greater than that of the S_2 peak.

The air temperature, relative air humidity, and wind speed spectra also showed daily fluctuations, usually with $S_1 > S_2$. Similarly, diurnal variations were observed for the barometric pressure, but with $S_2 > S_1$ (Table 2).

The transfer functions between the soil CO_2 efflux and each of the environmental variables were calculated to correlate the different time series and to provide some insights into the physical processes that were driving the cyclic behavior of the diffuse soil degassing. The correlation coefficient and the time delays between the variables monitored were calculated for the S_1 and S_2 peaks, taking into account only the correlation coefficients > 0.5. The prevailing correlations were recorded along with the barometric pressure, for both the S_1 and S_2 peaks, although the correlation with the S_2 period is greater ($r = 0.81$) (Table 3). If the transfer function is applied for different seasons, a greater correlation between the soil CO_2 efflux and the barometric pressure (essentially for the S_2 peak) is observed during the winter period. In the summer months, the air temperature also shows good correlation with the soil CO_2 efflux. The soil CO_2 efflux shows a delay of about 10 h to 11 h with the air temperature and wind speed, relative to the 24 h cycle (S_1). For the same period, the relative air humidity shows a negligible delay with the soil CO_2 efflux. Indeed, the inverse correlation detected between the CO_2 emission and the air temperature is in agreement with the higher CO_2 efflux observed in the morning and the lower CO_2 efflux observed in the early afternoon, contrary to what has been observed for biogenic environments [e.g., *Nakadai et al*., 2002].

4.3.1.2. The GFUR2 Data

Several technical problems affected station GFUR2 during the recording period, and for this reason, these data were split into four intervals to calculate the spectra. Daily variations are also observed in the soil CO_2 efflux time series recorded at station GFUR2, with the amplitude of the S_1 peak significantly higher than that of the S_2 peak. As an extreme case, during the winter months, only the S_1 peak is present (Figure 3 and Table S1 in the supporting information).

The air temperature, relative air humidity, wind speed, and barometric pressure time series recorded at station GFUR2 show daily fluctuations, with similar behaviors to those described for GFUR1 data. The transfer functions between the meteorological variables and the soil CO_2 efflux were also calculated for the data recorded at GFUR2 (Table S2 in the supporting information). For all of the periods, the air temperature, relative air humidity, and wind speed are the variables that best correlate with the soil CO_2 efflux for the S_1 peak, being the highest correlations identified during the summer periods. These correlations are also in

Table 3. Correlation and Time Delays (in hour) Between the Soil CO_2 Efflux and the Environmental Variables Registered at GFUR1 (Not Applicable: n.a.)

Soil CO_2 Efflux (g m^{-2} d^{-1})	2 October 2002 to 31 May 2006				Winter Period				Summer Period			
	Correlation (r)		Delay (h)		Correlation (r)		Delay (h)		Correlation (r)		Delay (h)	
Other Variables	1 cpd	2 cpd	1 cpd	2 cpd	1 cpd	2 cpd	1 cpd	2 cpd	1 cpd	2 cpd	1 cpd	2 cpd
Relative air humidity (%)	< 0.5	0.53	n.a.	~4 h	< 0.5	0.58	n.a.	~5 h	0.57	0.70	1–2 h	~4 h
Air temperature (°C)	< 0.5	0.68	n.a.	~2 h	< 0.5	0.75	n.a.	~2 h	0.76	0.79	10 h	~3 h
Barometric pressure (hPa)	0.71	0.81	~8 h	~5 h	0.65	0.86	~8 h	~5 h	0.86	0.88	~9 h	~6 h
Soil temperature (°C)	< 0.5	< 0.5	n.a.	n.a.	< 0.5	< 0.5	n.a.	n.a.	0.69	< 0.5	0 h	n.a.
CO_2 in the air (ppm)	0.53	< 0.5	0–1 h	n.a.	< 0.5	0.52	n.a.	~3 h	0.80	0.70	~1 h	0–1 h

©2014. American Geophysical Union. All Rights Reserved.

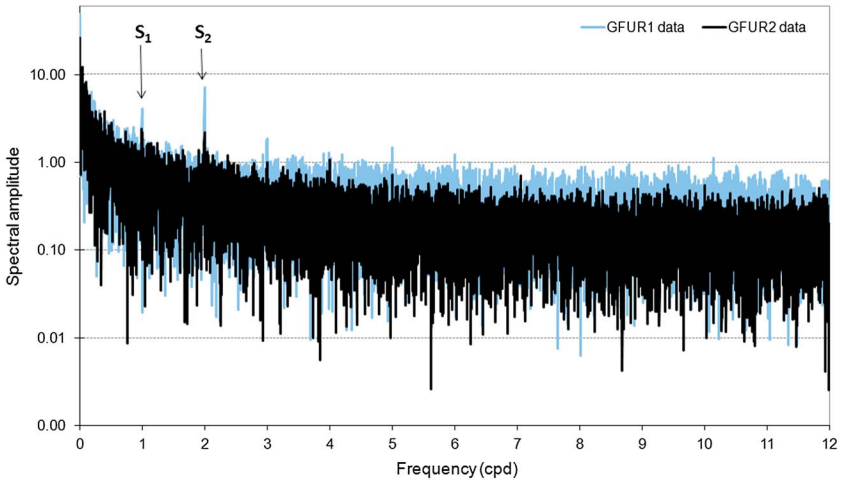

Figure 4. Spectral amplitude of the soil CO_2 efflux residuals obtained after applying MRA to the GFUR1 data for the period from 2 October 2002 to 31 May 2006 (blue) and to the GFUR2 data for the period between 1 January 2005 and 9 February 2007 (black).

agreement with the MRA models applied to the data, which showed that the wind speed and air temperature are the variables with the greatest influence on the CO_2 efflux variations [*Viveiros et al.*, 2008; *Viveiros*, 2010]. Unlike what was observed for GFUR1, for the data recorded at site GFUR2, the barometric pressure shows low correlation with CO_2 efflux. Regarding the delay between these variables, and as observed for GFUR1, the air temperature and wind speed show a 10 h to 11 h delay with the CO_2 efflux, while the relative air humidity is approximately in phase with the diurnal cycle of the gas flux.

4.3.1.3. The GFUR3 Data

Due to several technical problems that affected the GFUR3 station during the first year of data acquisition, only the data recorded between 8 August 2009 and 31 March 2010 were used to evaluate the daily cycles in the soil CO_2 efflux time series (Figure S1 in the supporting information). The spectrum of the soil CO_2 efflux does not show daily variations (Figure S2 in the supporting information). However, the spectrum of the data recorded for this site during August and September 2009 shows a weak S_1 component. In this case, the air temperature and wind speed also show a delay of about 10 h with the soil CO_2 efflux S_1 peak (Table S3 in the supporting information).

4.3.2. Soil CO_2 Efflux Residuals

The spectral analysis applied to the data sets confirmed some of the correlations established between the gas flux and environmental variables using MRA (see equations (1) to (3)). In fact, the MRA models highlight the significant influence of the barometric pressure on the gas flux at site GFUR1 and the air temperature at site GFUR2. These correlations are in agreement with the data obtained by applying the transfer function.

Calculation of the residuals obtained after applying MRA constitutes the best approach to infer the CO_2 input from depth. However, the spectra of the residuals still show S_1 and S_2 peaks, which are more evident for the GFUR1 residuals (Figure 4). These cycles are probably correlated with the environmental variables, and their presence shows that this MRA is not an efficient enough tool to filter out the influence of these external parameters on the gas flow, essentially for the data recorded at station GFUR1. Then, a second level of filter should be applied to the MRA residuals to remove the effects of the environmental variables. Such a filter might be a FFT low-pass filter with a cutoff frequency <1 cpd.

4.3.3. Long-Term Variations

Seasonal variations have been identified in the amount of CO_2 emitted at the permanent flux stations installed within the Furnas Volcano, with higher CO_2 efflux usually recorded during the winter months and lower values during the summer (Figure 5a) [*Viveiros et al.*, 2008, 2012].

Indeed, in addition to the diurnal cycles detected in the data sets, lower frequencies were identified in the CO_2 efflux time series (Figure 5b). The higher-energy peaks detected in the CO_2 efflux time series spectra correspond to a periodicity of ~ 340 days, and although this suggests spectral leakage, their amplitudes are higher than the daily peaks. The discrepancy observed between the 340 day and the 365 day annual band may result from a FFT resolution problem caused by the length of the analyzed time series. It would be necessary to use more data

©2014. American Geophysical Union. All Rights Reserved.

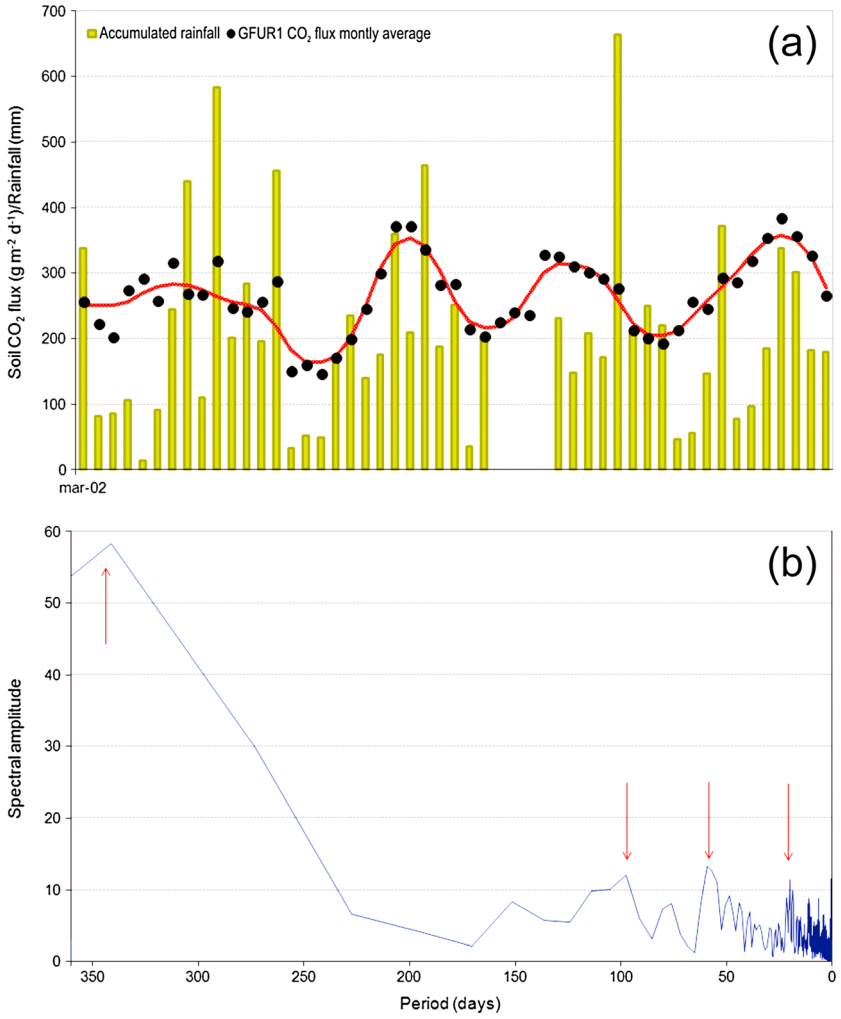

Figure 5. Seasonal trends of the soil CO_2 efflux. (a) Soil CO_2 efflux monthly means and the accumulated rainfall recorded at site GFUR1 from March 2002 to May 2006. (b) Amplitude spectrum showing the low-frequency peaks at GFUR1 for the period from 2 October 2002 to 31 May 2006. Red arrows identify the higher-energy peaks (period ~ 340, 98, 60, and 20 days).

points for the application of the FFT to have a shorter frequency point spacing, Δf, which corresponds to 1/(number of points for FFT × sampling rate in seconds) [*Schurig*, 2006]. Periodicities of ~ 98 days to 114 days, 55 days to 60 days, and 20 days to 28 days were also identified in the CO_2 efflux spectra of the permanent gas stations.

5. Numerical Simulations

Our goal was to simulate the effects produced by the atmospheric temperature and pressure changes on the observed CO_2 degassing variations. Several tests were performed with the Transport of Unsaturated Groundwater and Heat 2 (TOUGH2)/EOS2 fluid flow simulator [*Pruess et al.*, 1999], with a focus on 12 h and 24 h periods. We are aware that complex interactions between the various parameters are responsible for the observed CO_2 efflux cycles; nevertheless, we studied several parameters independently to provide insights into the individual contributions and to simplify the modeling approach. In particular, here we aimed to complete the simulations performed by *Rinaldi et al.* [2012] by (i) calculating the effects of a water-saturated layer that represents the water table at various depths, (ii) studying the effects of the amplitude of the air temperature diurnal perturbations, and (iii) detailing the effects of a thermal gradient in a gas-saturated system. Although we focused on the 12 h and 24 h periods, all of these effects can also be related to seasonal variations, since winter rainfalls raise the water table, lower (higher) surface temperature corresponds to a larger (smaller) temperature gradient within the soil, and diurnal air temperature amplitude changes with seasons.

©2014. American Geophysical Union. All Rights Reserved.

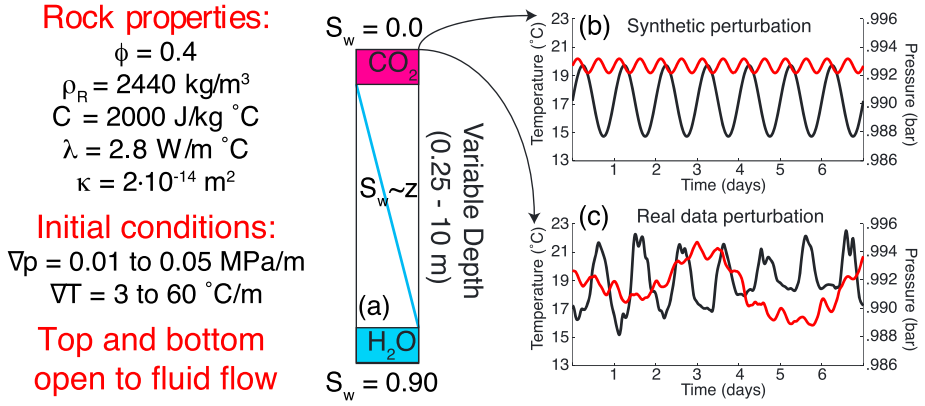

Figure 6. Computational domain and boundary conditions for one-dimensional simulations. (a) Initial phase condition for the two-phase, two-component case, with water saturation varying linearly from 0 to 0.9 at the water table depth (variable between 0.25 and 10 m). (b, c) Synthetic and real data for barometric pressure (red) and air temperature (black) perturbations applied at the top boundary. The rock properties were constant throughout the simulation, as listed. φ is the porosity, ρ is the rock density, λ is the thermal conductivity, C is the specific heat, and κ is the permeability.

As proposed by *Rinaldi et al.* [2012] the conceptual model assumes a CO_2 efflux fed by a pressurized hydrothermal reservoir at depth. We simulated a one-dimensional model with the following boundary conditions: open boundary with fixed pressure at the bottom of the domain, open boundary at the top of the domain with time-dependent barometric pressure and temperature, and closed side boundaries (Figure 6). The constant parameters of the model are listed in Figure 6. The variables of the system that we parameterized were the depth of the water table, the amplitude of the thermal perturbations, and the temperature at the water table depth (i.e., the thermal gradient). We performed the simulations for different pore pressure gradients of 0.01, 0.025, and 0.05 MPa/m, which were added to the hydrostatic pressure gradient and considered as constant in the system.

Time-dependent, 1 week long, barometric pressure and air temperature perturbations (either synthetic or from recorded data) were applied simultaneously at the top of the domain to simulate the atmospheric variations (Figures 6b and 6c for synthetic and real data perturbations, respectively).

To avoid superimposition of multiple effects on degassing, on the one side, we studied the effects of varying the depth of the water table (between 0.25 and 10 m), by simulating a two-component, two-phase system. In this case, the water saturation varied linearly from 0 at the top boundary (fully saturated with CO_2) to 0.9 at the depth of the water table (Figure 6a). On the other side, the surface temperature perturbation amplitude and the soil thermal gradient effects on the degassing are studied in a gas-saturated system.

In our simulations, the period of the atmospheric perturbations was too short to produce significant diffusion effects at the depths considered. As a consequence, CO_2 transfer is advection dominated. This advection can be driven by a pressure gradient, a temperature gradient, or both. As the temperature perturbations have a 24 h period, and the pressure perturbations have a 12 h period, the S_2/S_1 ratio for the 12 h over the 24 h flux components indicates whether the flow is mainly pressure driven ($S_2/S_1 > 1$) or temperature driven ($S_2/S_1 < 1$).

The effects of the depth of the water table on the degassing are shown in Figure 7 for both a real data atmospheric perturbation and a synthetic perturbation. We studied these effects on (a) the peak spectral amplitude of the S_1 and S_2 components (Figures 7a and 7c, for the real and the synthetic perturbations, respectively); (b) the ratio of the S_2 peak amplitude over the S_1 peak amplitude (Figures 7b and 7d, black lines); and (c) the mean degassing (Figures 7b and 7d, red lines) as a function of the depth of the water table in the range between 0.25 and 10 m. For these cases, we use a thermal gradient of 3°C/m. Results are compared to those of the previous gas-saturated approach (dashed lines) [*Rinaldi et al.*, 2012]. For all of the perturbations simulated (either real or synthetic), the general trend shows that the S_1 component is stronger than that of S_2 for a shallow water table (depth < 3 m) and that the S_2 component is dominant when the water table is at greater depths. In particular, the peaks of the S_1 component (Figures 7a and 7c, solid blue lines) are inversely correlated with the depth of the water table, and they are always smaller than in a gas-saturated

©2014. American Geophysical Union. All Rights Reserved.

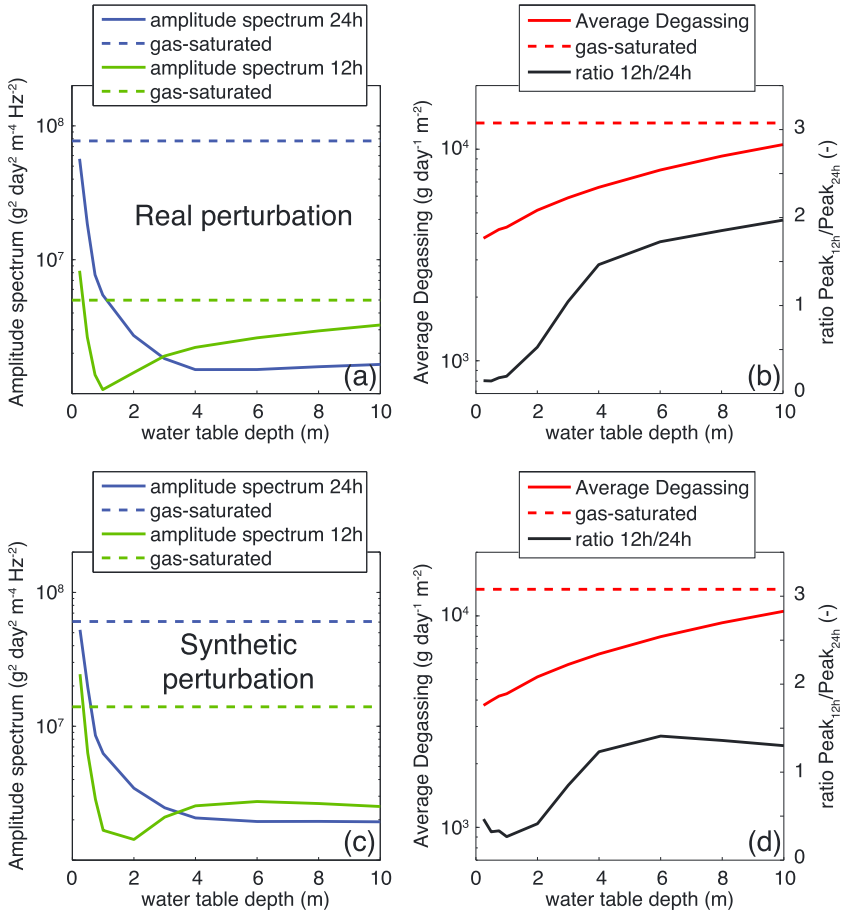

Figure 7. Effects of water saturation on peak amplitudes of diurnal (S_1) and semidiurnal (S_2) components and mean degassing. (a) S_1 (blue) and S_2 (green) peaks after simulation of a real (measured) multicomponent atmospheric perturbation at the top boundary; dashed lines represent the value for a gas-saturated system. (b) Mean degassing (red) and S_2/S_1 ratio (black) for a real data perturbation; red dashed line is the mean degassing for a gas-saturated system. (c) S_1 (blue) and S_2 (green) peaks after simulation of a synthetic (pure 12 h for pressure and pure 24 h for temperature) atmospheric perturbation at the top boundary. Dashed lines, value for a gas-saturated system; (d) mean degassing (red) and S_2/S_1 ratio (black) for a synthetic perturbation. Red dashed line is the mean amount of degassing for a gas-saturated system.

system (Figures 7a and 7c, dashed blue lines). The spectral amplitude peaks of the S_2 component (Figures 7a and 7c, solid green lines) first decrease for a very shallow water table and then logarithmically increase for a deeper water table. When compared to a gas-saturated system (Figures 7a and 7c, dashed green lines), S_2 is generally smaller, except for a very shallow water table. The minimum S_2 peak is observed at a water table depth that depends on the assigned perturbation at the top boundary. This minimum is at a depth of about 1 m for the real data (i.e., a multicomponent time series for both pressure and temperature), and it occurs at a depth of about 2 m for a clean, synthetic perturbation (pure 12 h for pressure and pure 24 h for temperature, with an amplitude similar to that of the real data). For both real and synthetic perturbations, the system switches from temperature-driven conditions ($S_1 > S_2$) to pressure-driven conditions ($S_1 < S_2$) when the water table is deeper than 3 m. The black solid lines in Figures 7b and 7d show the ratios between the amplitudes of these two components (S_2/S_1). This ratio depends on the assigned atmospheric perturbations (real data or synthetic). Both cases here show similar trends in the variation with a shallow water table, and while for a multicomponent perturbation (i.e., real data) the ratio increases for a deep water table (Figure 7b, solid black line), for a pure perturbation (i.e., synthetic), the ratio starts to decrease for a water table deeper than 6 m (Figure 7d, solid black line). The average degassing (Figures 7b and 7d, solid red lines) increases with the depth of the water table to tend toward a gas-saturated system (Figures 7b and 7d, dashed red lines). It is worth noting here that the average gas flux may increase by a factor of 3 when more gas is present in the system (i.e., when the water table is deeper).

©2014. American Geophysical Union. All Rights Reserved.

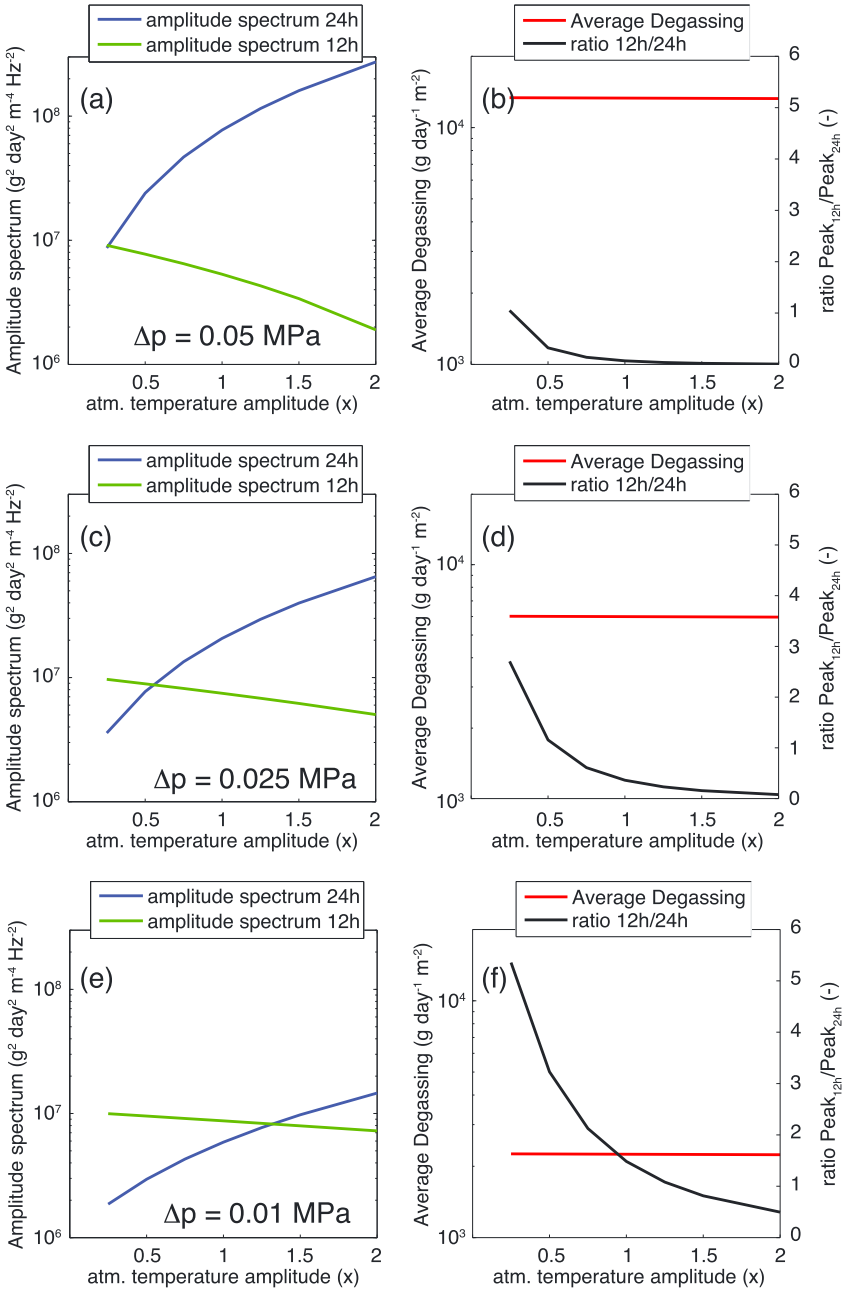

Figure 8. Effects of the amplitude of the air temperature perturbation on the peak amplitudes of diurnal (S_1) and semidiurnal (S_2) components and mean degassing. (a, c, and e) S_1 (blue) and S_2 (green) peak amplitudes for overpressure gradient 0.05, 0.025, and 0.01 MPa/m, respectively; (b, d, and f). Mean degassing (red) and ratio (S_2/S_1: black) for overpressure gradient 0.05, 0.025, and 0.01 MPa/m, respectively.

All the above mentioned results are found by applying a pressure gradient of 0.05 MPa/m greater than the hydrostatic one. The same results are found by varying the pressure gradient in the system, with effects only on the effective peak values and the mean degassing.

The second parameter that we studied was the amplitude of the air temperature perturbations, which can depend on the site and on the season. The effects of this parameter were studied by simulating a 1 m deep, gas-saturated system with gradient of 3°C/m and three different values for the pressure gradient (0.01, 0.025, and 0.05 MPa/m). In our simulations, the air temperature amplitude varied between 0.25 and twofold the amplitude recorded over 1 week at GFUR2 [*Rinaldi et al.*, 2012, Figure 6b]. For this case study, we simulated a

©2014. American Geophysical Union. All Rights Reserved.

Table 4. Summary of the Main Frequencies Identified in the Soil CO_2 Efflux Time Series According to the Defined Global Phenomena

Monitoring Sites	Periodicity (days)	Global Phenomena With Similar Periodicity	Season
GFUR1	~340	Solar cycle (~ 365 days)	-
	98	Madden-Julian Oscillation (30–100 days)[a]	-
	60	Solar cycle (multiple of solar rotation ~26 days)[b] Madden-Julian Oscillation (30–100 days)[a]	-
	20–23	Earth tides (Lunar cycles: ~ 15/29 days)[c]	-
	1	Diurnal cycle (24 h) (S_1)[c]	Summer
	0.5	Semidiurnal cycle (12 h) (S_2)[c]	Summer and winter
GFUR2	~340	Solar cycle (~ 365 days)	-
	114	Madden-Julian Oscillation (30–100 days)[a]	
	55–60	Solar cycle (multiple of solar rotation ~ 26 days)[b] Madden-Julian Oscillation (30–100 days)[a]	-
	22–28	Earth tides (lunar cycle: ~ 15/29 days)[c]	-
	1	Diurnal cycle (24 h) (S_1)[c]	Summer and winter
	0.5	Semidiurnal cycle (12 h) (S_2)[c]	Summer
GFUR3	1	Diurnal cycle (24 h) (S_1)[c]	Summer

[a]Bibliographic reference: *Groves-Kirkby et al*. [2006].
[b]Bibliographic reference: *Han and Han* [2002].
[c]Bibliographic reference: *Schureman* [1976].

few values for the pressure as the resulting trends might vary substantially. Results show that for all of the pressure gradient values, the amplitude of the diurnal S_1 component always increases with the amplitude of the air temperature (Figures 8a, 8c, and 8e, blue lines). In contrast, the semidiurnal component (S_2) produced by the atmospheric pressure variations always decreases with the amplitude of the air temperature (Figures 8a, 8c, and 8e, green lines). Hence, the S_2/S_1 ratio decreases with the amplitude of the air temperature (Figures 8b, 8d, and 8f, black lines). The transition from a S_2-dominant (pressure-driven) to a S_1-dominant (temperature-driven) system occurs at an amplitude of the air temperature perturbation that depends on the pore pressure gradient: the larger the pore pressure gradient, the lower the amplitude needed for the transition (0.25 times for 0.05 MPa/m, ~0.5 times for 0.025 MPa/m, and ~1.25 times for 0.01 MPa/m, Figures 8a, 8c, and 8e). It is worth noting that the air temperature amplitude does not affect the mean degassing (Figures 8b, 8d, and 8f, red lines).

Finally, we also studied the effects of the soil temperature gradient on the CO_2 efflux. Simulations were performed using a 1 m deep, gas-saturated domain, similar to that presented by *Rinaldi et al*. [2012]. However, we introduced a significant difference between the air and soil temperatures and considered diverse gradients from 3 to 60°C/m. These show that both the S_1 and S_2 components decrease with the temperature gradient, for all of the pressure gradients (0.05, 0.025, and 0.01 MPa). These results for different pressure gradients are similar to those obtained by *Rinaldi et al*. [2012] that used a given overpressure.

6. Discussion

6.1. Soil CO_2 Efflux Daily Oscillations

The spectral analysis applied to the soil CO_2 efflux time series highlights the presence of diurnal and seasonal variations. The gas flux signals include several high- and low-frequency peaks, as summarized in Table 4. Daily cycles are observed in the soil CO_2 efflux time series recorded at stations GFUR1 and GFUR2, where two dominant spectral peaks are identified for the 24 h (S_1) and the 12 h (S_2) components during the summer months. During the winter period, only one daily component is observed, as S_1 and S_2, for sites GFUR2 and GFUR1, respectively. In the particular case of station GFUR3, the data show periodic behavior (S_1) during the summer months only.

The daily cycles recognized in the meteorological variables suggest that the CO_2 efflux variations are dependent on the atmospheric cycles. The transfer functions applied to each of the meteorological variables and to the soil CO_2 efflux show that the air temperature, relative air humidity, and wind speed correlate well with the diurnal peak; for the GFUR1 data, the semidiurnal oscillations in CO_2 efflux essentially correlate with the barometric pressure, which is characterized by a strong 12 h period cycle. This correlation disappears at GFUR2, which confirms the study of *Viveiros et al*. [2008] that showed that the influence of the environmental variables on the gas flux is highly site dependent.

©2014. American Geophysical Union. All Rights Reserved.

Even during stable weather conditions (e.g., dry days with small variations in barometric pressure), the daily soil gas flux varies significantly by 10 to 20% around the mean value at all of the permanent stations. The CO_2 efflux usually reaches its maximum at dawn, and as the Sun rises, it decreases to reach a minimum at around noon (12:00–14:00). Thereafter, the CO_2 emissions again increase to reach a second daily maximum at sunset and a minimum around midnight. In fact, the S_1 peaks observed for the soil CO_2 efflux time series showed a delay of about 10 h to 11 h with the wind speed and air temperature diurnal cycles at all of the monitoring sites, in agreement with the high soil CO_2 efflux values recorded in the early morning and the low soil CO_2 efflux in the early afternoon. These inverse correlations observed between the CO_2 emission and the air temperature/wind speed are also compatible with results obtained previously using MRA at station GFUR2 [*Viveiros et al*., 2008]. From these correlations it becomes evident that the CO_2 released in these hydrothermal areas behaves contrary to that in areas with a source of biogenic CO_2 only, where the production is positively correlated with air/soil temperature changes [*Bajracharya et al*., 2000; *Nakadai et al*., 2002; *Raich and Potter*, 1995; *Witkamp*, 1969]. The magnitude of the diurnal variations in the soil CO_2 efflux at the Furnas Volcano stations (usually from 50 to 100 g m^{-2} d^{-1}) excludes the possibility that the variations in CO_2 have a biogenic origin. Studies performed in biogenic environments [e.g., *Nakadai et al*., 2002] report daily amplitudes for CO_2 efflux of about 5 to 6 g m^{-2} d^{-1}, which are 1 order of magnitude lower than the data in the present study, which are clearly dominated by the volcanic/hydrothermal environment [*Viveiros et al*., 2010, 2012]. Differences observed in the CO_2 efflux behavior in hydrothermal/biogenic environments may also provide ways to identify the origin of the CO_2 when isotopic data are not available and/or when the CO_2 effluxes are very low.

These daily cycles are also in agreement with the data obtained by *Rinaldi et al*. [2012] that modeled the influences of barometric pressure and air temperature on gas flux fluctuations. They show the practically inverse correlation between CO_2 efflux and air temperature, as well as the correlation with the 12 h barometric pressure cycle. In *Rinaldi et al*. [2012], the simulation results confirmed that the pressure changes at the soil-air interface can pump out and press in the soil gases, not only in the surface layer, as this can also propagate to the interior of the domain. *Rinaldi et al*. [2012] highlighted the role of the air temperature in the fluid mobility, as a temperature drop should increase the fluid density, and hence the fluid flow, according to the Darcy flow equation. In addition to the pressure gradient created close to the surface by the air temperature/barometric pressure diurnal cycles, the wind speed may also interfere with the gas fluxes. Considering that the air temperature cycles are in phase with the wind speed variable, the lower air temperature/wind speed values recorded during the night may also contribute to the increase in the CO_2 emissions.

The seasonal patterns for the diurnal and semidiurnal components are highlighted in the spectrograms of the soil CO_2 efflux that were recorded at stations GFUR1 and GFUR2. The S_1 peak correlates well with the air temperature, relative air humidity, and wind speed, and it is dominant in the soil CO_2 efflux signal during the summer months at both sites GFUR1 and GFUR2 and during the winter period at station GFUR2. The S_2 component prevails over the S_1 component for the soil CO_2 efflux time series recorded at station GFUR1 during the winter months. The differences observed for these two monitoring sites may be correlated with the gas reservoir overpressure. As demonstrated by *Rinaldi et al*. [2012], when the degassing shows mainly the semidiurnal component, this may be connected to a lower gas reservoir overpressure. This could also be in agreement with the values observed, as the mean soil CO_2 efflux and temperatures recorded at station GFUR1 (267 g m^{-2} d^{-1}) are lower than at GFUR2 (398 g m^{-2} d^{-1}), which probably indicate a lower gas overpressure.

6.2. Comparison With Numerical Models

Our data obtained here with different water saturation profiles (Figure 7) indicate a predominance of S_1 for shallow depths of the water table, which agree well with the data recorded at site GFUR2. At GFUR2, where the water table is at about 1 m in depth, the S_1 component is predominant in both the dry and wet seasons, while S_2 disappears during the winter. Although S_2 does not disappear completely from the numerical model, the results show the minimum amplitude of S_2 at about 1 m depth, which corresponds to the characteristics observed at site GFUR2.

The lower S_1 component observed at station GFUR1 compared to station GFUR2 is probably due to smaller gas overpressure at GFUR1, which is confirmed by a lower observed average flux. This is in agreement with the modeling results [*Rinaldi et al*., 2012, Figures 8a, 8c, and 11d], where the lower the overpressure, the lower the S_1 amplitude.

©2014. American Geophysical Union. All Rights Reserved.

According to our models, any drop in the water table in the first 10 m would be accompanied by an increase in the mean CO_2 efflux. This is a consequence of an increase in fluid mobility in the upper system (i.e., less dense fluid), due to water withdrawal. As shown in Figure 7a, a system with a deepening water table tends to a gas-saturated system, as modeled by *Rinaldi et al.* [2012]. However, in the Azores (in the present study), as in Campi Flegrei [*Granieri et al.*, 2010], higher gas fluxes are observed in the winter periods, during which the water table is high. This discrepancy between the observations and the atmospheric effects modeling would indicate that the seasonal modulation of the mean degassing is not a surficial effect but has a deeper origin. In consequence, the likely cause of the higher degassing in winter is the infiltration of meteoric water inside the hydrothermal system, which will enhance the convection and the transfer of CO_2-rich hydrothermal fluids to the surface.

Based on the records at the monitored sites, higher air temperature amplitudes are observed during the summer months (Table S4 in the supporting information), which perfectly agrees with the higher amplitudes of S_1 during this period, as shown by the model (Figure 8). The S_2 component decreases slightly along the range assumed for the amplitude variation. Even if the air temperature amplitude influences the amplitude of the diurnal cycles, the mean degassing is almost constant and does not appear to depend on this variable. *Steinitz et al.* [2007] recognized similar observations for a ^{222}Rn time series showing that the magnitude of the diurnal components reflects seasonal patterns.

Preliminary spectral analysis of the data acquired by other permanent flux stations installed in the Azores has also been performed to compare with the results obtained for the Furnas permanent stations (Table S5 in the supporting information). The Terceira station (GTER1) was installed in the Furnas do Enxofre fumarolic field, which is located in the central part of the Terceira Island at about 600 m altitude and where CO_2 effluxes oscillate around a mean of 330 g m^{-2} d^{-1} [*Ferreira et al.*, 2005]. The spectral content shows a weak S_1 peak only during the summer months (May to September). The acyclic CO_2 time series recorded at station GTER1 may be hypothetically explained by the extreme weather conditions at this site, with high wind speeds and intense rainfall that can mask any small oscillations in the gas concentration. However, this behavior, which is similar to the data recorded at station GFUR3, highlights that both of these stations are located at advection-dominated points with anomalously high soil temperature (at 30 cm depth the temperature is >30°C). In addition, previous data [*Rinaldi et al.*, 2012] have shown lower degassing with higher temperatures in the system, since higher temperature corresponds to a lower fluid density and so less degassing (Darcy equation). Even if additional studies need to be done, this can contribute to the explanation that the annual cycles with low CO_2 effluxes are usually recorded during the summer months, and higher CO_2 fluxes are recorded during the winter period.

A permanent station installed in the Furna do Enxofre lava cave (GGRC1, Graciosa Island) is also located in a thermally anomalous zone with a mean CO_2 efflux around 4400 g m^{-2} d^{-1} [*Ferreira et al.*, 2005]. Gas flux time series show a predominant S_2 peak during the different seasons, which correlates well with the barometric pressure, similar to what was observed at station GFUR1. The weak S_1 component in the CO_2 effluxes recorded at GGRC1 may be explained by the absence of insolation (the station is located inside a lava cave), with a consequently smaller effect of the S_1 air temperature cycle. *Perrier and Girault* [2013] showed that the S_2 peak is indeed essentially due to the influence of the atmospheric pressure.

Finally, our simulation results (former and current) show the significant impact that not only the meteorological variables but also the soil conditions can have on the soil CO_2 efflux periodicity and degassing. However, care needs to be taken, because the models presented here are introduced as partial explanations for the CO_2 efflux variations observed, and extra modeling is necessary to better show the differences in the degassing cycles. For instance, one aspect that needs to be taken into account in future studies is the importance of inserting interfaces in the soil and to not only consider models based on a homogeneous half-space [*Perrier and Girault*, 2013].

6.3. Soil CO_2 Efflux Seasonal Oscillations

There are also low-frequency peaks in the spectra of the soil CO_2 efflux, namely, the existence of annual cycles (of ~340 days) (Table 4). Considering the length of the available data set (maximum 37,000 hourly entries for site GFUR1), the determination of these low-frequency peaks was not as precise as for the higher-frequency peaks, and longer time series would be necessary to properly record the seasonal variations. Even though, *Reboita* [2004] defined annual cycles of 300 to 400 days with influences from several atmospheric phenomena (e.g., air temperature and humidity) and 340 days was the period for the barometric pressure; these parameters could in part contribute to explain the periodicities observed.

©2014. American Geophysical Union. All Rights Reserved.

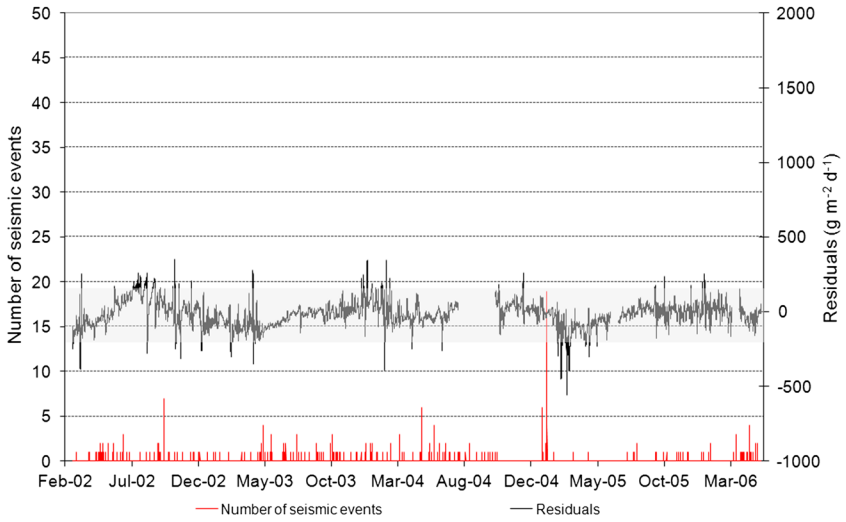

Figure 9. GFUR1 soil CO_2 efflux residuals and hourly seismic events recorded at Furnas Volcano between March 2002 and May 2006 (CVARG/CIVISA database). Gray band: the interval $\mu \pm 2\sigma$ ($-16 \pm 2 \times 82$).

Notwithstanding the difficulty in the definition of the number of days for the annual cycles, differences of about 100 and 200 g m^{-2} d^{-1} are observed in the mean CO_2 effluxes between the winter and summer periods. Despite the significant variations detected in the CO_2 emissions for the different seasons, the mean annual CO_2 efflux is constant through the years (Figure 5) [*Viveiros et al*., 2012]. This suggests that the differences identified in the CO_2 emissions between the winter and summer periods do not result from changes in the deep volcanic source but from efflux modulation that is due to the aquifer seasonal variations.

Other low frequencies were also identified in the CO_2 efflux time series recorded at stations GFUR1 and GFUR2, namely, at 20 to 28 days and at 55 to 60 days. The 20 to 28 days cycle can be correlated with the lunar cycles that can potentially interfere with the gas flux. Some discrepancies in the day's periodicity may still be caused by the resolution of the spectral analysis and/or by a leakage effect.

In line with the 55 to 60 days periodicity, *Marques* [2013] also identified a 60 day periodicity in a 31 yearlong rainfall time series that was recorded by a meteorological station located near to Furnas Lake. This periodicity is coincident with the CO_2 efflux variations observed at the Furnas permanent stations, which may be correlated with the strong influence of the rainfall on the gas flux fluctuations [*Viveiros et al*., 2008]. The 60 day cycle may also result from a multiple of the solar rotation, even if the correlation between solar activity and CO_2 efflux periodicity remains to be clarified. Recently, *Nicholson et al*. [2013] identified dominant cycles of an approximately 50 day period in the SO_2 flux time series recorded at Soufrière Hills (Montserrat), as well as some periods with intervals of 11 to 14 days and 17 to 26 days. These coincident periods may represent common driven mechanisms, and they need to be better investigated to learn more about the underlying control of the volcanic behavior. Despite these differences of some days in the periodicities identified in the CO_2 efflux time series recorded at sites GFUR1 and GFUR2, the general cycles are similar, which suggest that there is a common driving mechanism to explain the CO_2 efflux variations. Longer data sets and evaluation of the relationships between CO_2 effluxes and ocean/lunar tides are needed to better interpret the CO_2 periodicities observed.

6.4. Filtered CO_2 Efflux Time Series and Correlation With Seismic Activity

Time series featuring periodicities and correlations with environmental variables need to be filtered using MRA and low-pass FFT. The filtered time series, or residuals, constitute the best representation of the deep-CO_2 signals, and these must be the ones used in volcano monitoring programs. If the resulting CO_2 efflux time series approaches a normal distribution, then $\mu \pm 2\sigma$ can be used as the interval that comprises "normal" gas flux variations (where μ is the mean and σ the standard deviation). Any values falling outside of this range (as outliers) may indicate changes in the deep hydrothermal system (Figures 9 and 10). In the particular case of station GFUR3, and considering that the diurnal periodicities in the gas flux time series were identified over 2 months only, the FFT filter was not applied to these data.

©2014. American Geophysical Union. All Rights Reserved.

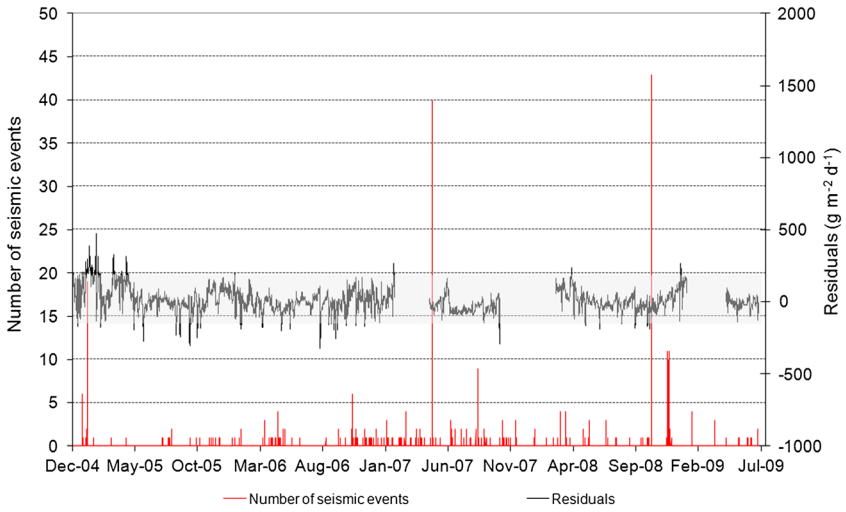

Figure 10. GFUR2 soil CO_2 efflux residuals and the hourly seismic events recorded at Furnas Volcano between January 2005 and June 2009 (CVARG/CIVISA database). Gray band: the interval $\mu \pm 2\sigma$ ($10 \pm 2 \times 78$).

In the present study, the computed CO_2 residuals are compared with the number of seismic events recorded in the Furnas Volcano area, and the soil CO_2 efflux time series recorded at stations GFUR1 and GFUR2 do not appear to be directly correlated with the periods of seismicity. There was also no evident correlation between the CO_2 residuals and the periods when the higher magnitude seismic events occurred (2 February 2005 and 4 November 2006), even if some outliers were identified in the data recorded at GFUR2 in the beginning of February 2005 (Figure 10). This behavior was not observed in the GFUR1 data, and similar spiky outliers are observed at GFUR2 during periods without seismic activity. In fact, care must be taken here, as some periods during which the CO_2 residuals fall outside the defined variability band may potentially be due to periods of extreme weather conditions that were not totally filtered by the defined algorithms.

Richon et al. [2003] identified a geochemical anomaly before a magnitude 7 seismic event at the Taal Volcano (Philippines), by recognizing that in the period preceding the seismic event, the S_2 component disappeared from the ^{222}Rn signal and reappeared after the earthquake. This study showed that the identification of a geochemical anomaly may not only depend on the increase/decrease in the variables analyzed but may also be related to changes in the periodicity of the gas geochemical time series. In fact, models presented by *Rinaldi et al.* [2012] confirmed that the unrelated evolution of the diurnal components could indicate changes in the source conditions and not only changes in the soil permeability. Even if no significant increase/decrease in the soil CO_2 efflux time series that can be associated to deep changes were observed in the present study, spectrograms still show some small variations. The S_1 component is significantly weaker in the spectrogram of station GFUR2 between 15 October and 20 December 2008 (Figure S3 in the supporting information), and it is temporally coincident with the seismic swarm with a higher number of seismic events recorded at the Furnas Volcano during the period monitored and with a maximum 2.1 M_D on 16 October 2008 (CVARG/CIVISA database). Variations in the air temperature, relative air humidity, and wind speed are not the explanation for these changes, as diurnal cycles are still identified for this period (Table S1 in the supporting information). The differences in the behavior of the S_1 peak suggest changes in the deep system making this study suitable for the use of changes in the spectrograms as an extra tool to evaluate the occurrence of changes in volcano/hydrothermal systems.

7. Conclusions

Despite the increasing number of studies that focus on the cyclic behavior of geophysical data, there are very few in the literature that have analyzed the periodic variations in soil CO_2 efflux in hydrothermal environments. In the present study, we observed diurnal and semidiurnal periodicities in the CO_2 efflux recorded at permanent stations installed on the Azores archipelago, and we related these to the effects of periodic surface temperature and pressure changes using linear Fourier analysis, considering that the frequencies of the perturbations

©2014. American Geophysical Union. All Rights Reserved.

induced on the efflux are the same as those on the atmospheric perturbation signals. As a forthcoming step, wavelet analysis might supplement our approach, by investigating the nonlinear responses of the system at different timescales. Seasonal cycles were also identified in the soil CO_2 emissions, and despite some discrepancies observed between the different monitoring sites, in general, higher CO_2 efflux values were recorded in the early morning (daily cycles) and during the rainy months (seasonality). Recognition and understanding of the CO_2 periodic behavior and establishment of correlations with environmental variables have implications for any seismovolcanic monitoring program, which highlights once again the importance of the integration of gas geochemical data with other external variables (e.g., environmental phenomena). In addition, quantification of the daily and seasonal CO_2 variations is important to understand the "natural" variability of CO_2 emission and contributes to an understanding of the intrasurvey and intersurvey variability. In the present study, the CO_2 effluxes varied by up to 200 g m^{-2} d^{-1} just due to seasonal effects.

Hydrothermal CO_2 efflux atmospheric-induced variations are opposite to those observed in biogenic environments, and thus, they can also be used to infer the origin of the CO_2 released (i.e., biogenic versus hydrothermal). This is especially helpful for low-CO_2 degassing areas and for where no carbon isotope information is available. Even if the hydrothermal CO_2 effluxes are dominant in the Furnas monitored sites when compared to the biogenic CO_2 emission, future studies should also quantify the contribution of the soil respiration [*Maier et al*., 2010, 2011] to understand the effects of the biological activity at each monitoring site.

Granieri et al. [2003] also identified the diurnal S_1 peak in CO_2 efflux time series recorded at the Solfatara volcano, and recently, *Hernández et al*. [2012] identified the same diurnal cycle in data recorded on the Lanzarote Island (Canary Islands). *Padrón et al*. [2008] also recognized diurnal and semidiurnal fluctuations in the gas flux assessed in 2004 for a station located on El Hierro Island (Canary Islands). These above mentioned studies only suggested that CO_2 efflux periodicities are related to the air temperature and barometric pressure cycles without any attempts to model these phenomena. *Rinaldi et al*. [2012] provided the first study in which diurnal cycles for CO_2 emitted in hydrothermal environments were modeled. The present study provides an additional contribution to the understanding of the degassing behavior in volcanic/hydrothermal areas by also simulating the influence of the water table depth, the amplitude of the thermal perturbations, and the soil thermal gradients in a gas-saturated system. Simulations can be extended to other degassing areas, and the numerical results show that the simulated parameters can explain the daily diurnal and semidiurnal variations observed in CO_2 efflux time series for different season and for different stations. However, additional work needs to be done to model the seasonal effects on the degassing, as the surficial processes used both in this study and by *Rinaldi et al*. [2012] are not enough to fully simulate some of the observed variations.

As mentioned above, the recognition of periodic variations that are mostly correlated with environmental phenomena once again highlights the need to apply filters to various monitoring data. In fact, this study suggests two-step filtering based on MRA and FFT filters that may result in a final time series for the CO_2 efflux variations that best represent the deep changes (i.e., seismic and/or volcanic activity). Even if in the present study no correlation can be established between CO_2 efflux residuals and the seismic activity recorded at Furnas Volcano, changes in the CO_2 efflux daily periodicities were detected in the last trimester of 2008, and in the same period there were high number of seismic events that affected the area. Considering that this lack of periodic behavior is not explained by the monitored atmospheric variables, the variations may be caused by changes in the source conditions and are likely to be triggered by seismic or volcanic activity.

Acknowledgments

The data that support this study were recorded by the permanent stations installed in the Azores archipelago, which are under the propriety of the CVARG/CIVISA. The gas monitoring activities were funded both by the Regional Civil Protection and by private companies (e.g., EDA Renováveis), and for this reason these data can only be released under request and with approval of the above mentioned institutions. F. Viveiros is supported by a PostDoctoral grant from Fundo Regional da Ciência, Região Autónoma dos Açores (PROEMPREGO Operational Program). A.P. Rinaldi is currently supported by DOE-LBNL contract DE-AC02-05CH11231. This study was supported by the Azores Regional Government/Serviço Regional de Protecção Civil e Bombeiros dos Açores, in the scope of the scientific and technical protocols to guarantee the Azores Seismovolcanic Surveillance and the Emergency Planning Studies. This study was also a part of the MED-SUV project, which received funding from the European Union Seventh Programme for Research, Technological Development and Demonstration under grant agreement 308665. The authors would like to thank Pedro Hernàndez and an anonymous reviewer for their comments and suggestions that improved the quality of this paper.

References

Aumento, F. (2002), Radon tides on an active volcanic island: Terceira, Azores, *Geof. Int*., *41*(4), 499–505.

Bajracharya, R. M., R. Lal, and J. M. Kimble (2000), Diurnal and seasonal CO_2-C flux from soil as related to erosion phases in Central Ohio, *Soil Sci. Soc. Am. J*., *64*, 286–293.

Bettencourt, M. L. (1979), O clima de Portugal Fascículo XVIII. O clima dos Açores como recurso natural, especialmente em agricultura e indústria do turismo [in Portuguese], Instituto Nacional de Meteorologia e Geofísica, p. 72.

Carapezza, M. L., T. Ricci, M. Ranaldi, and L. Tarchini (2009), Active degassing structures of Stromboli and variations in diffuse CO_2 output related to the volcanic activity, *J. Volcanol. Geotherm. Res*., *182*, 231–245.

Chiodini, G., R. Cioni, M. Guidi, B. Raco, and L. Marini (1998), Soil CO_2 flux measurements in volcanic and geothermal areas, *Appl. Geochem*., *13*, 543–552.

Chiodini, G., F. Frondini, C. Cardellini, D. Granieri, L. Marini, and G. Ventura (2001), CO_2 degassing and energy release at Solfatara volcano, Campi Flegrei, Italy, *J. Geophys. Res*., *106*, 16,213–16,221.

Cigolini, C., et al. (2009), Radon surveys and real-time monitoring at Stromboli volcano: Influence of soil temperature, atmospheric pressure and tidal forces on ^{222}Rn degassing, *J. Volcanol. Geotherm. Res*., *184*, 381–388.

©2014. American Geophysical Union. All Rights Reserved.

Clements, W. E., and M. H. Wilkening (1974), Atmospheric pressure effects on ^{222}Rn transport across the Earth-air interface, *J. Geophys. Res.*, *79*(33), 5025–5029.
Cole, P., G. Queiroz, N. Wallenstein, J. L. Gaspar, A. Duncan, and J. Guest (1995), An historic subplinian/phreatomagmatic eruption: The 1630 AD eruption of Furnas Volcano, São Miguel, Azores, *J. Volcanol. Geotherm. Res.*, *69*, 117–135.
Crosta, G. B., and P. Dal Negro (2003), Observations and modelling of soil slip-debris flow initiation processes in pyroclastic deposits: The Sarno 1998 event, *Nat. Hazard Earth Syst. Sci.*, *3*, 53–69.
Cruz, J. V., P. Freire, and A. Costa (2010), Mineral waters characterization in the Azores archipelago (Portugal), *J. Volcanol. Geotherm. Res.*, *190*, 353–364.
DROTRH/INAG (2001), Plano Regional da Água [in Portuguese], Tech. Rep., DROTRH-INAG, 575 pp., Ponta Delgada, Portugal.
Esposito, L., and F. M. Guadagno (1998), Some special geotechnical properties of pumice deposits, *Bull. Eng. Geol. Environ.*, *57*, 41–50.
Ferreira, T., J. L. Gaspar, F. Viveiros, M. Marcos, C. Faria, and F. Sousa (2005), Monitoring of fumarole discharge and CO_2 soil degassing in the Azores: Contribution to volcanic surveillance and public health risk assessment, *Ann. Geophys.*, *48*(4–5), 787–796.
Granieri, D., G. Chiodini, W. Marzocchi, and R. Avino (2003), Continuous monitoring of CO_2 soil diffuse degassing at Phlegraean Fields (Italy): Influence of environmental and volcanic parameters, *Earth Planet. Sci. Lett.*, *212*, 167–179.
Granieri, D., R. Avino, and G. Chiodini (2010), Carbon dioxide diffuse emission from the soil: Ten years of observations at Vesuvio and Campi Flegrei (Pozzuoli), and linkages with volcanic activity, *Bull. Volcanol.*, *72*, 103–118, doi:10.1007/s00445-009-0304-8.
Groves-Kirkby, C. J., A. R. Denman, R. G. M. Crockett, P. S. Phillips, and G. K. Gillmore (2006), Identification of tidal and climatic influences within domestic radon time-series from Northamptonshire, UK, *Sci. Total Environ.*, *367*, 191–202.
Guest, J., J. L. Gaspar, P. D. Cole, G. Queiroz, A. M. Duncan, N. Wallenstein, T. Ferreira, and J. M. Pacheco (1999), Volcanic geology of Furnas Volcano, São Miguel, Azores, *J. Volcanol. Geotherm. Res.*, *92*, 1–29.
Han, Y., and Y. Han (2002), Time variations of the near 5-month period of sunspot numbers, *Chin. Sci. Bull.*, *47*(23), 1969–1973, doi:10.1360/02tb9427.
Harris, F. J. (1978), On the use of windows for harmonic analysis with the discrete Fourier transform, *Proc. IEEE*, *66*, 51–83.
Hernández, P. A., et al. (2012), Analysis of long- and short-term temporal variations of the diffuse CO_2 emission from Timanfaya volcano, Lanzarote, Canary Islands, *Appl. Geochem.*, *27*(12), 2486–2499.
Hinkle, M. E. (1990), Factors affecting concentrations of helium and carbon dioxide in soil gases, in *Geochemistry of Gaseous Elements and Compounds*, edited by E. M. Durrance et al., pp. 421–448, Theophrastus Publ., S. A., Athens.
Hinkle, M. E. (1991), Seasonal and geothermal production variations in concentrations of He and CO_2 in soil gases, Roosevelt Hot Springs Known Geothermal Resource Area, Utah, U.S.A., *Appl. Geochem.*, *6*, 35–47.
Hinkle, M. E. (1994), Environmental conditions affecting of He, CO_2, O_2 and N_2 in soil gases, *Appl. Geochem.*, *9*, 53–63.
Klusman, R. W., and J. D. Webster (1981), Preliminary analysis of meteorological and seasonal influences on crustal gas emission relevant to earthquake prediction, *Bull. Seismol. Soc. Am.*, *71*(1), 211–222.
Klusman, R. W., J. N. Moore, and M. P. LeRoy (2000), Potential for surface gas flux measurements in exploration and surface evaluation of geothermal resources, *Geothermics*, *29*, 637–670.
Lewicki, J. L., G. E. Hilley, T. Tosha, R. Aoyagi, K. Yamamoto, and S. M. Benson (2007), Dynamic coupling of volcanic CO_2 flow and wind at the Horseshoe Lake tree kill, Mammoth Mountain, California, *Geophys. Res. Lett.*, *34*, L03401, doi:10.1029/2006GL028848.
López, D. L., J. Bundschuh, G. J. Soto, J. F. Fernandez, and G. E. Alvarado (2006), Chemical evolution of thermal springs at Arenal volcano, Costa Rica: Effect of volcanic activity, precipitation, seismic activity, and Earth tides, *J. Volcanol. Geotherm. Res.*, *157*, 166–181.
Maier, M., H. Schack-Kirchner, E. E. Hildebrand, and J. Holst (2010), Pore-space CO_2 dynamics in a deep, well-aerated soil, *Eur. J. Soil Sci.*, *61*, 877–887, doi:10.1111/j.1365-2389.2010.01287.x.
Maier, M., H. Schack-Kirchner, E. E. Hildebrand, and D. Schindler (2011), Soil CO_2 efflux vs. soil respiration: Implications for flux models, *Agric. Forest Meteorol.*, *151*, 1723–1730, doi:10.1016/j.agrformet.2011.07.006.
Marques, R. (2013), Estudo de movimentos de vertente no concelho da Povoação (ilha de São Miguel, Açores): Inventariação, caracterização e análise da susceptibilidade [in Portuguese], Unpublished PhD thesis, p. 455, Univ. of the Azores, Portugal.
Marques, R., J. Zêzere, R. Trigo, J. Gaspar, and I. Trigo (2007), Rainfall patterns and critical values associated with landslides in Povoação County (São Miguel Island, Azores): Relationships with the North Atlantic Oscillation, *Hydrol. Process*, *22*, 478–494, doi:10.1002/hyp.6879.
Martini, F., C. Bean, G. Saccorotti, F. Viveiros, and N. Wallenstein (2009), Seasonal cycles of seismic velocity variations detected using coda wave interferometry at Fogo volcano, São Miguel, Azores, during 2003–2004, *J. Volcanol. Geotherm. Res.*, *181*, 231–246.
Marzocchi, W., G. Vilardo, D. P. Hill, P. Ricciardi, and C. Ricco (2001), Common features and peculiarities of the seismic activity at Phlegraean Fields, Long Valley, and Vesuvius, *Bull. Seismol. Soc. Am.*, *91*(2), 191–205.
Nakadai, T., M. Yokozawa, H. Ikeda, and H. Koizumi (2002), Diurnal changes of carbon dioxide flux from bare soil in agricultural field in Japan, *Appl. Soil Ecol.*, *19*, 161–171.
Nicholson, E., T. A. Mather, D. M. Pyle, H. M. Odbert, and T. Christopher (2013), Cyclical patterns in volcanic degassing revealed by SO_2 flux time series analysis: An application to Soufrière Hills Volcano, Montserrat, *Earth Planet. Sci. Lett.*, *375*, 209–221.
Padrón, E., G. Melián, R. Marrero, D. Nolasco, J. Barrancos, G. Padilla, P. A. Hernandéz, and N. M. Pérez (2008), Changes in the diffuse CO_2 emission and relation to seismic activity in and around El Hierro, Canary Islands, *Pure Appl. Geophys.*, *165*, 95–114.
Patanè, D., M. Mattia, G. Di Grazia, F. Cannavò, E. Giampiccolo, C. Musumeci, P. Montalto, and E. Boschi (2007), Insights into the dynamic processes of the 2007 Stromboli eruption and possible meteorological influences on the magmatic system, *Geophys. Res. Lett.*, *34*, L22309, doi:10.1029/2007GL031730.
Perrier, F., and F. Girault (2013), Harmonic response of soil radon-222 flux and concentration induced by barometric oscillations, *Geophys. J. Int.*, *195*(2), 945–971.
Pinault, J.-L., and J.-C. Baubron (1996), Signal processing of soil gas radon, atmospheric pressure, moisture, and soil temperature data: A new approach for radon concentration modelling, *J. Geophys. Res.*, *101*(B2), 3157–3171.
Pinault, J.-L., and J.-C. Baubron (1997), Signal processing of diurnal and semidiurnal variations in radon and atmospheric pressure: A new tool for accurate in situ measurement of soil gas velocity, pressure gradient, and tortuosity, *J. Geophys. Res.*, *102*(B8), 18,101–18,120.
Pruess, K., C. M. Oldenburg, and G. Moridis (1999), TOUGH2 user's guide, version 2.0, Paper LBNL-43134, Lawrence Berkeley Natl. Lab., Berkeley, Calif.
Raich, J. W., and C. S. Potter (1995), Global patterns of carbon dioxide from soils, *Global Biogeochem. Cycles*, *9*(NO1), 23–36.
Reboita, M. S. (2004), Elementos da variabilidade climática no extremo sul do Brasil, no período de 1990 a 2001 [in Portuguese], Master thesis, p. 211, Univ. Federal do Rio Grande, Brasil.
Richon, P., J.-C. Sabroux, M. Halbwachs, J. Vandemeulebrouck, N. Poussielgue, J. Tabbagh, and R. Punongbayan (2003), Radon anomaly in the soil of Taal volcano, the Philippines: A likely precursor of the M7.1 Mindoro earthquake (1994), *Geophys. Res. Lett.*, *30*(9), 1481, doi:10.1029/2003GL016902.

©2014. American Geophysical Union. All Rights Reserved.

Richon, P., F. Perrier, E. Pili, and J.-C. Sabroux (2009), Detectability and significance of 12 hr barometric tide in radon-222 signal, dripwater flow rate, air temperature and carbon dioxide concentration in an underground tunnel, *Geophys. J. Int.*, *176*, 683–694, doi:10.1111/j.1365-246X.2008.04000.x.

Richon, P., F. Perrier, B. P. Koirala, F. Girault, M. Bhattarai, and S. N. Sapkota (2011), Temporal signatures of advective versus diffusive radon transport at a geothermal zone in Central Nepal, *J. Environ. Radioact.*, *102*, 88–102.

Rigby, J. G., and D. D. La Pointe (1993), Wind and barometric pressure effects on Radon in two mitigated houses, The 1993 International Radon Conference, 61–68.

Rinaldi, A. P., J. Vandemeulebrouck, M. Todesco, and F. Viveiros (2012), Effects of atmospheric conditions on surface diffuse degassing, *J. Geophys. Res.*, *117*, B11201, doi:10.1029/2012JB009490.

Robinson, A. L., R. G. Sextro, and W. J. Riley (1997), Soil-gas entry into houses driven by atmospheric pressure fluctuations—The influence of soil properties, *Atmos. Environ.*, *31*(10), 1487–1495.

Rogie, J. D., D. M. Kerrick, M. L. Sorey, G. Chiodini, and D. Galloway (2001), Dynamics of carbon dioxide emission at Mammoth Mountain, California, *Earth Planet. Sci. Lett.*, *188*, 535–541.

Schureman, P. (1976), *Manual of Harmonic Analysis and Prediction of Tides*, *U.S. Dept. of Commerce, Coast and Geodetic Survey, Spec. Publ. 98*, U.S. Government Printing Office, Washington, D. C.

Schurig, D. (2006), Off-normal incidence simulations of metamaterials using FDTD, *Int. J. Numer. Model.*, *19*, 215–228.

Searle, R. (1980), Tectonic pattern of the Azores spreading centre and triple junction, *Earth Planet. Sci. Lett.*, *51*, 415–434.

Silva, R., M. Bonagura, N. Damiano, D. Zandomeneghi, G. Saccorotti, N. Wallenstein, A. Quadrio, and E. Carmona (2004), Preliminary results of a seismic experiment in Fogo and Furnas volcanoes, São Miguel Island (Azores), Portugal, Proceedings of the 4th Assembleia Luso-Espanhola de Geodesia e Geofísica, 343–344.

Silva, R., J. Havskov, C. Bean, and N. Wallenstein (2012), Seismic swarms, fault plane solutions and stress tensors for São Miguel Island central region (Azores), *J. Seismol.*, *16*, 389–407, doi:10.1007/s10950-012-9275-x.

Steinitz, G., O. Piatibratova, and S. M. Barbosa (2007), Radon daily signals in the Elat Granite, southern Arava, Israel, *J. Geophys. Res.*, *112*, B10211, doi:10.1029/2006JB004817.

Stolte, J. (1997), Determination of the saturated hydraulic conductivity using the constant head method, in *Manual for Soil Physical Measurements*, *Tech. Doc.*, vol. 37, edited by J. Stolte, DLO Winand Staring Centre, Wageningen, Netherlands.

Van Camp, M., and P. Vauterin (2005), Tsoft: Graphical and interactive software for the analysis of time series and Earth tides, *Comput. Geosci.*, *31*(5), 631–640.

Vauterin, P., and M. Van Camp (2008), TSoft manual version 2.1.2 Release date 04-08-2008, Royal Observatory of Belgium, Bruxelles, 58 pp.

Viveiros, F. (2010), Soil CO_2 flux variations at Furnas Volcano (São Miguel Island, Azores), Unpublished PhD thesis, p. 266, Univ. of the Azores, Portugal.

Viveiros, F., T. Ferreira, J. Cabral Vieira, C. Silva, and J. L. Gaspar (2008), Environmental influences on soil CO_2 degassing at Furnas and Fogo volcanoes (São Miguel Island, Azores archipelago), *J. Volcanol. Geotherm. Res.*, *177*, 883–893.

Viveiros, F., T. Ferreira, C. Silva, and J. L. Gaspar (2009), Meteorological factors controlling soil gases and indoor CO_2 concentration: A permanent risk in degassing areas, *Sci. Total Environ.*, *407*, 1362–1372.

Viveiros, F., C. Cardellini, T. Ferreira, S. Caliro, G. Chiodini, and C. Silva (2010), Soil CO_2 emissions at Furnas Volcano, São Miguel Island, Azores archipelago: Volcano monitoring perspectives, geomorphologic studies and land use planning application, *J. Geophys. Res.*, *115*, B12208, doi:10.1029/2010JB007555.

Viveiros, F., C. Cardellini, T. Ferreira, and C. Silva (2012), Contribution of CO_2 emitted to the atmosphere by diffuse degassing from volcanoes: The Furnas Volcano case study, *Int. J. Global. Warming*, *4*(3/4), 287–304.

Witkamp, M. (1969), Cycles of temperature and carbon dioxide evolution from litter and soil, *Ecology*, *50*(5), 922–924.

©2014. American Geophysical Union. All Rights Reserved.